

The Higher Oxides of Carbon $C_{8n}O_{2n}$ ($n = 3-5$): Synthesis, Characterization, and X-ray Crystal Structure. Formation of Cyclo[n]carbon Ions C_n^+ ($n = 18, 24$), C_n^- ($n = 18, 24, 30$), and Higher Carbon Ions Including C_{60}^+ in Laser Desorption Fourier Transform Mass Spectrometric Experiments

Yves Rubin,¹ Michael Kahr,² Carolyn B. Knobler,¹ François Diederich,^{*1} and Charles L. Wilkins^{*2}

Contribution from the Department of Chemistry and Biochemistry, University of California, Los Angeles, California 90024-1569, and the Department of Chemistry, University of California, Riverside, California 92521. Received May 4, 1990.
Revised Manuscript Received September 10, 1990

Abstract: The new higher oxides of carbon **1** ($C_{24}O_6$), **2** ($C_{32}O_8$), and **3** ($C_{40}O_{10}$) have been prepared from the macrocyclic ketals **5-7** and characterized as stable colored solids. The electronic absorption spectra of the carbon oxides **1-3** differ from those of the ketals **5-7**. The absorption bands of **1-3** are broader and shifted to longer wavelength. The X-ray crystal structure of oxide **1** has been determined, showing that **1** is planar, with bent diyne units. The laser desorption Fourier transform mass spectra of **1** and **2** show a remarkable ease of successive losses of two CO molecules to give C_{18} and C_{24} ions, respectively, in both positive and negative modes. The C_{30} ion formed by fragmentation of oxide **3** is considerably less stable than the smaller homologues and is only observed in the negative ion mode. In the positive ion spectra recorded at low desorption laser power, ions corresponding to the dimers of the cyclocarbons are observed. In addition, higher carbon ions are formed with C_{60}^+ being abundant in the spectra obtained from all three carbon oxides. The ion distributions at high laser power correlate with previous observations on the laser desorption of graphite and other carbon-rich materials. Besides a strong C_{60}^+ ion, carbon ions up to C_{400}^+ are abundant under these conditions in all spectra.

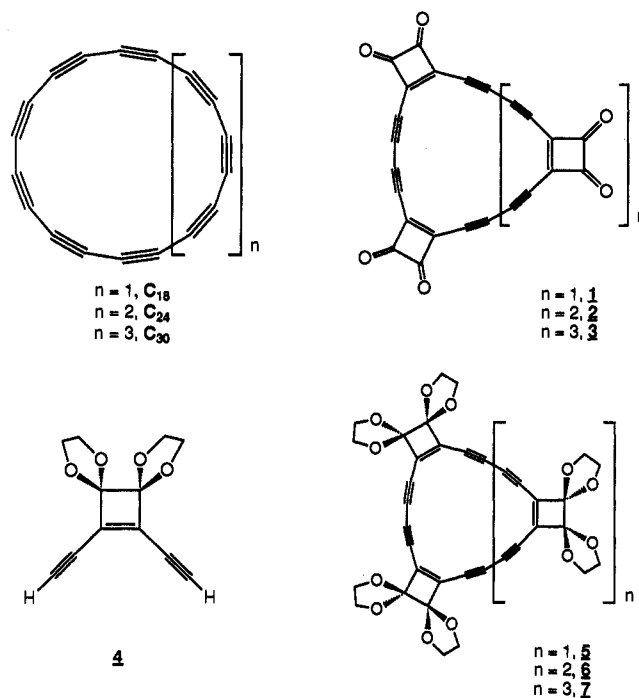
Introduction

In our previous publications, we reported the synthesis of the macrocyclic ketals **5-7** and showed that the deprotection of **5** and **6** in concentrated sulfuric acid led smoothly to solutions of the protonated oxides of carbon **1** and **2** (Scheme I).^{3,4} In this paper, we describe an improved preparation of the dehydroannulenes **5-7**, as well as the synthesis and full characterization of $C_{24}O_6$ (**1**), $C_{32}O_8$ (**2**), and $C_{40}O_{10}$ (**3**), by far the largest carbon oxides ever prepared. The X-ray crystallographic structure of the smallest oxide **1** has been obtained, thus confirming the identity of these new compounds. In the following, the fragmentation patterns of the carbon oxides **1-3** under various conditions are investigated by laser desorption Fourier transform mass spectrometry (LD/FTMS).⁵ These studies show that **1-3** are ideal precursors to the cyclo[n]carbons C_{18} , C_{24} , and C_{30} .⁶ Interesting fragmentations and condensations, with or without concomitant rearrangements, are also observed, leading to carbon ions of lower and higher masses.

Results and Discussion

Synthesis. The Hay coupling reaction of the bisketal **4** to yield the three cyclobutenodehydroannulenes **5-7** could be considerably improved by adding a molar equivalent instead of a catalytic amount of $CuCl \cdot TMEDA$ ($TMEDA = N,N,N',N'$ -tetramethylethylenediamine) to the solution of **4** in acetone.⁴ The reaction time shortened from 2 days to 2 hours, and the isolated yields of the macrocyclic bisketals **5**, **6**, and **7** were 16%, 18%, and 7%, respectively. Consequently, the total cyclization yield was im-

Scheme I



proved from previously 10% to 41%. As reported before, the deprotection of the three ketals **5-7** in 96% sulfuric acid proceeded within a few minutes to give solutions of the protonated carbon oxides **1-3**. Attempted isolation of the products by dropping the sulfuric acid solutions into a stirred mixture of ice-water and dichloromethane led to the isolation of only minor quantities of the expected products, large amounts of polymers being formed by the reaction of water with these seemingly strong Michael acceptors. After considerable experimentation with a number of reagents including trifluoroacetic acid and trifluoromethanesulfonic acid,⁴ the successful isolation of **1**, **2**, and **3** was accomplished by

(1) University of California, Los Angeles.
 (2) University of California, Riverside.
 (3) Rubin, Y.; Diederich, F. *J. Am. Chem. Soc.* **1989**, *111*, 6870-6871.
 (4) Rubin, Y.; Knobler, C. B.; Diederich, F. *J. Am. Chem. Soc.* **1990**, *112*, 1607-1617.
 (5) For a recent review, see: Nuwaysir, L. M.; Wilkins, C. L. In *Lasers and Mass Spectrometry*; Lubman, D. L., Ed.; Oxford University Press: New York, 1990; pp 291-315.
 (6) For another precursor leading to neutral C_{18} , see: Diederich, F.; Rubin, Y.; Knobler, C. B.; Whetten, R. L.; Schriver, K. E.; Houk, K. N.; Li, Y. *Science* **1989**, *245*, 1088-1090.

Table I. ^{13}C NMR Chemical Shifts (ppm) of the Carbon Oxides **1**, **2**, and **3**

compound	$\text{C}\equiv\text{C}-\text{C}=\text{C}$	$\text{C}\equiv\text{C}-\text{C}=\text{C}$	$\text{C}=\text{C}$	$\text{C}=\text{O}$
(a) In D_2SO_4				
1	83.0	108.8	180.9	194.6
2	81.7	107.8	180.0	194.5
3	81.5	106.9	176.8	194.4
(b) In Organic Solvents				
1 ^a	84.5 (84.1) ^d	107.7 (106.3)	180.8 (179.1)	192.3 (191.2)
2 ^b	82.7 (82.2) ^d	107.7 (104.9)	180.0 (177.8)	191.1 (190.7)
3 ^c	82.0	106.1	176.2	190.3

^a In nitrobenzene- d_5 , solvent peak as reference. ^b In 1,1,2,2-tetrachloroethane- d_2 , solvent peak as reference. ^c In CDCl_3 , solvent peak as reference. ^d Values in 2-methyltetrahydrofuran in parentheses, internal Me_4Si as reference.

direct extraction of their sulfuric acid solutions with 1,2-dichloroethane. In the clear, colored solutions obtained (orange-yellow, red, and yellow, respectively), the carbon oxides were partially protonated, as demonstrated by the presence of a very strong peak at m/z 97 (HSO_4^-) in the negative ion LD/FTMS spectra of these solutions. Treatment of the solutions of **1**–**3** with anhydrous K_2CO_3 or with MgO led to an instantaneous formation of black polymers. However, powdered CaCO_3 was effective in removing any traces of acids without simultaneously decomposing compounds **1**–**3**. At this stage, the peak at m/z = 97 in the negative ion LD/FTMS spectra had completely disappeared. It is interesting to note that although other chlorinated solvents such as dichloromethane or chloroform were as effective as 1,2-dichloroethane in extracting the oxides **2** and **3** (but not **1**), they also extracted much more sulfuric acid into the organic phase. Benzene could also be used to extract **1** and **3**, but not **2**. However, benzenesulfonic acid was formed as a byproduct in this process, as shown by ^1H and ^{13}C NMR. The yields of the oxides **1**–**3** after evaporation of the solvent and drying were consistently above 70% and up to 99%, showing the surprising mildness of concentrated sulfuric acid as a deprotection reagent for **5**–**7**.

Properties of the Carbon Oxides. The identity of **1** and **2** is demonstrated by the X-ray crystal structure for **1** (see below) as well as by their spectral data. In particular, both compounds have parent negative ions in the LD/FTMS spectra (see below), and their ^{13}C NMR spectra are very characteristic. Besides two types of acetylenic carbons, the only other absorptions are due to the cyclobutenedione system. Although compound **3** does not show a parent ion in both positive and negative LD/FTMS spectra, characteristic fragments resulting from **3** ($\text{C}_{40}\text{O}_{10}$) corresponding to six, seven, and eight losses of carbon monoxide (i.e., $\text{C}_{34}\text{O}_4^-$, $\text{C}_{33}\text{O}_3^-$, $\text{C}_{32}\text{O}_2^-$), respectively, are present along with a strong C_{30} negative ion. This and very similar ^{13}C NMR and IR spectra of **3** to those of compounds **1** and **2** and the identical method of formation of all these compounds from the completely characterized⁴ precursors **5**–**7** strongly support the structural identity assigned to **3**.

The carbon oxides **1**–**3** are quite stable as solutions in dry nonnucleophilic solvents or in the solid state. However, on exposure to daylight, dilute solutions of **1**–**3** rapidly lose their color and their characteristic absorption bands in the electronic absorption spectra (Figure 2) to give a low-intensity, featureless absorption curve tailing down to 800 nm. On attempted melting point determination, compounds **1**–**3** exploded violently above 85 °C. Traces of nucleophiles, including water, led to rapid polymerization.

As expected, the proton NMR spectra of **1**–**3** were free of any absorption other than solvent signals. The ^{13}C NMR spectral data are shown in Table I. The chemical shifts of the unprotonated materials in organic solvents do not differ dramatically from the values measured previously in D_2SO_4 for the protonated oxides.⁴

The infrared spectra for **1**–**3** were recorded in chloroform solutions since rapid decomposition and absorption broadening was observed in KBr. The remarkable simplicity of these spectra reflects the high symmetry of the carbon oxide molecules. Characteristic absorptions in the spectra of **1**, **2**, and **3** are the strong $\text{C}=\text{O}$ stretching bands at 1791, 1787, and 1787 cm^{-1} ,

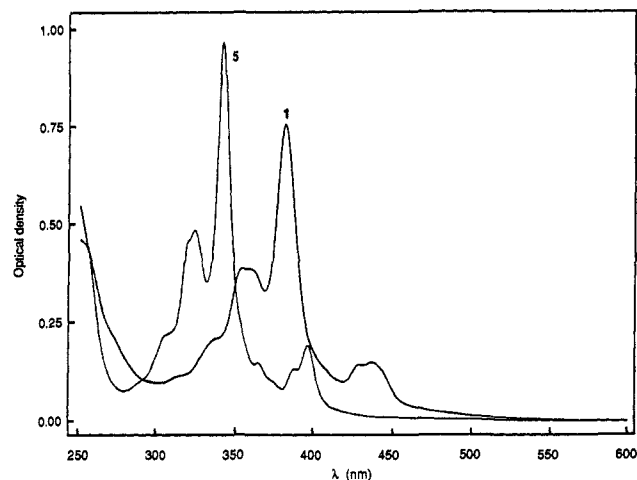


Figure 1. Electronic absorption spectra of **1** and **5** recorded in 1,2-dichloroethane for **1** and in dichloromethane for **5**: $T = 293$ K, $d = 1$ cm, $c = 1.2 \times 10^{-5}$ M for **1** and $c = 1.4 \times 10^{-5}$ M for **5**.

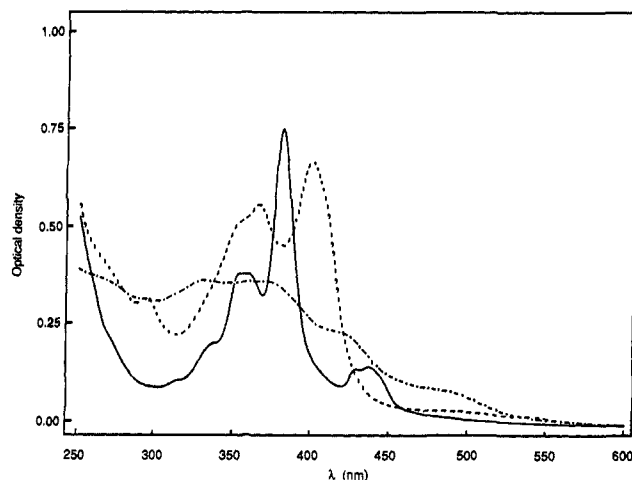


Figure 2. Electronic absorption spectra of **1**–**3** recorded in 1,2-dichloroethane: $T = 293$ K, $d = 1$ cm, $c = 1.2 \times 10^{-5}$ M for **1** (—), $c = 1.0 \times 10^{-5}$ M for **2** (---), and $c = 1.1 \times 10^{-5}$ M for **3** (···).

together with the weak $\text{C}\equiv\text{C}$ stretching bands at 2129, 2125, and 2125 cm^{-1} , respectively.

As for the ketals **5**–**7**, the electronic absorption spectra of the carbon oxides **1**–**3** are very informative of their conformation in solution.⁷ In particular, the spectra for the diatropic [18]annulene **5** and the corresponding oxide **1** are very similar (Figure 1). The large bathochromic shifts (~ 40 nm) for the absorption bands of **1**, as compared to **5**, show extended conjugation of the annulene perimeter through the carbonyl groups. The well-structured absorption curve recorded for **1** and **5** is highly indicative of a planar, rigid annulene perimeter.⁷ The almost perfect planarity of the 18-membered ring in **1** is demonstrated by the X-ray crystal structure discussed below. In the electronic absorption spectrum of the 24-membered annulene **2**, a decreased stability of the planar conformation must be taken in account, since the absorption bands are broadened when compared to those of the [18]annulene **1** (Figure 2). In addition, the molar extinction coefficient for the major band in the spectrum of **2** is reduced. This is in sharp contrast to the relation between the spectra of hexaketals **5** and octaketals **6**. In the ketal series, both [18]- and [24]annulene chromophores prefer a rigid planar conformation.⁷ Their electronic absorptions show highly resolved vibrational structure, and the bands of the more extended perimeter **6** have considerably higher molar extinction coefficients. Similar to the ketal **7**, the larger

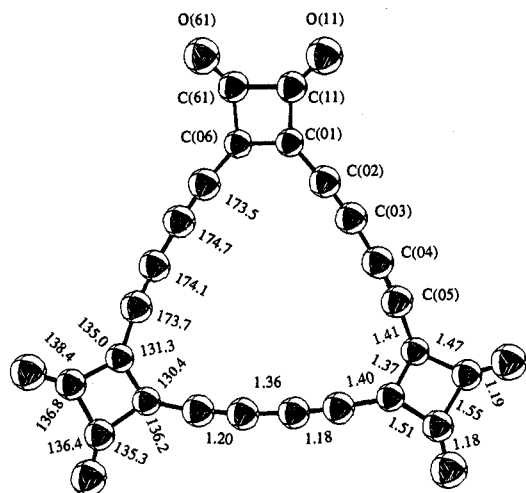


Figure 3. X-ray crystal structure of **1** with front view, above, and edge view, below.

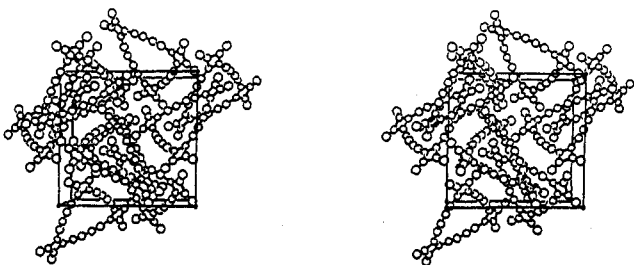


Figure 4. Stereoview of the crystal packing diagram for compound **1**. Solvent molecules have been removed for clarity.

oxide **3** shows a featureless spectrum indicative of a high conformational flexibility of this [30]annulene perimeter.

X-ray Crystal Structure of the Carbon Oxide $C_{24}O_6$ (1**).** Crystals of **1** were grown by diffusion-crystallization of the compound in 1,2-dichloroethane/hexane. The deep red parallelepipeds were kept at 25 °C in the dark over 2 weeks, without apparent decomposition. The X-ray diffraction was conducted at 25 °C with the crystal sealed in a glass capillary with the crystallization solvent. The oxide **1** crystallizes in the cubic space group $P2_13$ with $a = 14.4209(10)$, $V = 2999 \text{ \AA}^3$, and an occupation of four molecules in the unit cell.⁸ The molecule has a crystallographic 3-fold axis. Two crystallographically different areas contain poorly characterized solvent. The solvent occupies nearly one-third of the volume of the crystal.

As seen in Figure 3, the structure of the oxide **1** is attractive by its symmetry. Strain in the molecule is expressed in the considerable bending of the three diyne units and in the reduced value of the internal C—C=C angle at the cyclobutenedione units. The C(04)–C(05)–C(06) angle of 173.5 (16)° is the smallest in the diyne units. The C(02)–C(01)–C(06) and C(05)–C(06)–C(01) angles at the fused cyclobutenedione units are 131.3 (13)° and 130.4 (12)°, respectively. They are much smaller than the corresponding angles (135.4 (6)° and 133.6 (6)°, respectively) in 3,4-bis(phenylethynyl)-3-cyclobutene-1,2-dione (**8**) whose X-ray crystal structure is shown in Figure 5.⁹ The observed strain

(8) Data were collected at 25 °C on a Syntex PI diffractometer modified by Professor C. E. Strouse, UCLA, using $CuK\alpha$ radiation, $2\theta \leq 115^\circ$, giving 787 unique reflections; the structure was solved by statistical methods (SHELX86), yielding $R = 0.102$, $R_w = 0.104$ for 445 reflections with $I > 3\sigma(I)$. Disordered solvent prevented further refinement.

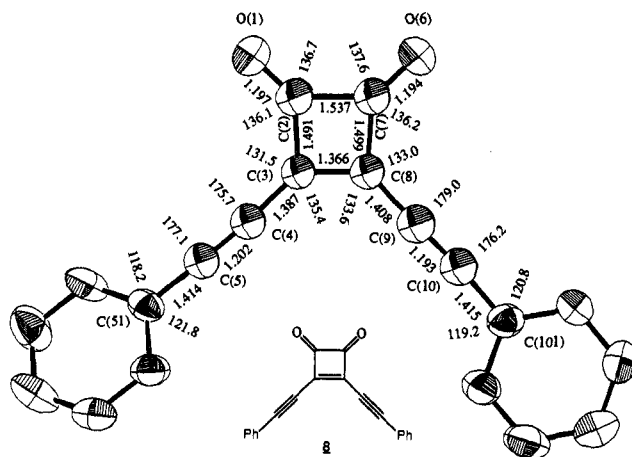


Figure 5. X-ray crystal structure of **8**.

pattern in **1** has been correctly predicted by AM1 and MM2 calculations on related systems.⁷

The 18-membered carbon cycle in **1** is planar; the maximum distance of a carbon to the least-squares plane through the C_{18} ring is 0.05 (1) Å. The oxygen atoms show the largest deviation from the least-squares plane through the entire molecule; in each cyclobutenedione unit, the two oxygen atoms are 0.22 (1) Å away on opposite sides of the plane (Figure 3, lower). The four-membered rings are planar within 0.02 (1) Å and are tilted 2.2° with respect to the plane of the 18-membered ring. The crystal packing diagram in Figure 4 shows the low efficiency of packing in the crystal. The molecules of **1** are placed in an edge-to-face-type array, leaving a large empty portion of space for disordered solvent.

Laser Desorption Fourier Transform Mass Spectroscopy

Negative Ion Spectra. Although clear discernible fragmentation patterns attributable to the parent carbon oxides are evident in both negative ion and positive ion spectra, the negative ion laser desorption spectra of **1**, **2**, and **3** are less ambiguous, due to the absence of ions attributable to higher carbon aggregates, which complicate the positive ion spectra. Both the hexaketone **1** and the octaketone **2** spectra reveal the presence of a molecular anion (m/z 384 and m/z 512, respectively) in addition to abundant ions arising from loss of even numbers of carbonyls (Figure 6). The C_{18} anion (m/z 216) resulting from loss of all six carbonyls is a prominent fragment of oxide **1**, and the C_{24} anion arising from loss of all eight carbonyls is the major product of oxide **2** fragmentation. These observations are in accord with the expected stability of the C_{18} and C_{24} molecules^{6,10–13} and the ready loss of CO in other cyclobutenediones.^{4,14} However, in dramatic contrast, the negative ion laser desorption FT mass spectrum of the larger oxide **3** with a 30-carbon ring contains no evidence of a molecular anion and shows extensive fragmentation leading to carbon anions from C_5 to C_{33} , indicative of the instability of the C_{30} fragment anion (Figure 7).^{10,15,16} Thus, although the C_{30} , $C_{33}O_2$, $C_{33}O_3$, and $C_{34}O_4$ anions are clearly present in the spectrum, the most abundant anion is the m/z 120 species C_{10} , probably arising from further decomposition of the 30-carbon ring. Interestingly, the even-numbered carbon fragments appear associated with a pre-

(9) X-ray crystal data of **8** ($C_{20}H_{10}O_2$), $M_r = 282.3$; monoclinic; space group = $P2_1/a$; $Z = 4$; a (Å) = 7.498 (1); b (Å) = 11.473 (2); c (Å) = 17.607 (3); $\beta = 96.189$ (4)°; $V = 1506 \text{ \AA}^3$. Data were collected at 25 °C on a Syntex PI diffractometer modified by Professor C. E. Strouse, UCLA, using $CuK\alpha$ radiation, to a maximum $2\theta = 100^\circ$, giving 1547 unique reflections, and the structure was solved by statistical methods. The final discrepancy index was $R = 0.090$, $R_w = 0.120$ for 1343 independent reflections with $I > 3\sigma(I)$.

(10) Hoffmann, R. *Tetrahedron* **1966**, *22*, 521–538.
 (11) Bernholz, J.; Phillips, J. C. *J. Chem. Phys.* **1986**, *85*, 3258–3267.
 (12) Pitzer, K. S.; Clementi, E. *J. Am. Chem. Soc.* **1959**, *81*, 4477–4485.
 (13) Parent, D. C.; McElvany, S. W. *J. Am. Chem. Soc.* **1989**, *111*, 2393–2401.
 (14) Bock, H.; Ried, W.; Stein, U. *Chem. Ber.* **1981**, *114*, 673–683.
 (15) Yang, S.; Taylor, K. J.; Craycraft, M. J.; Conceicao, J.; Pettiette, C. L.; Cheshnovsky, O.; Smalley, R. E. *Chem. Phys. Lett.* **1988**, *144*, 431–436.
 (16) Weltner, W., Jr.; Van Zee, R. *J. Chem. Rev.* **1989**, *89*, 1713–1747.

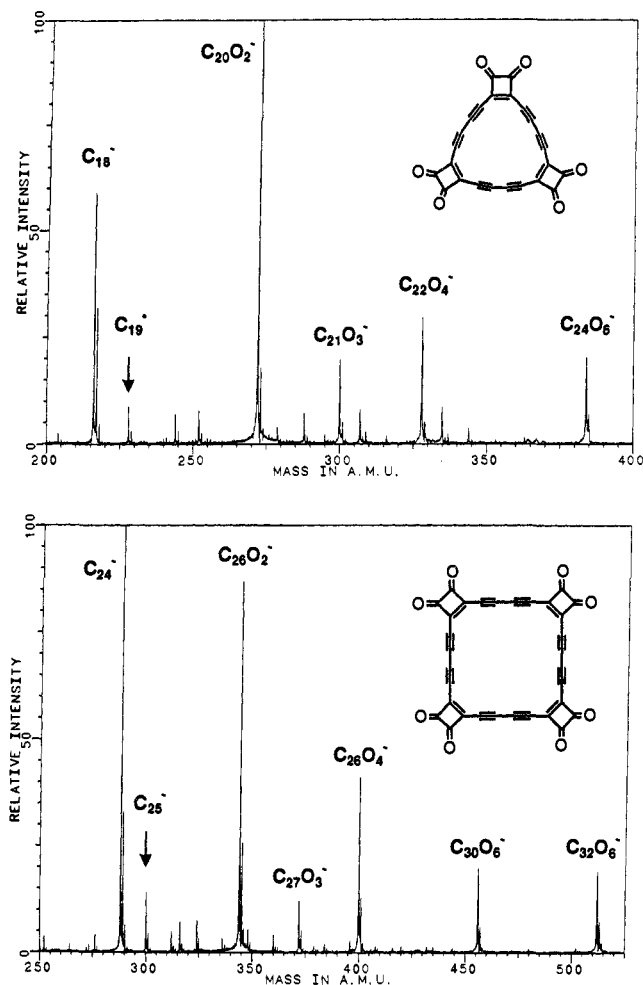


Figure 6. Negative ion laser desorption Fourier transform mass spectra of carbon oxides 1 and 2 at low laser power.

dominant peak bearing one extra hydrogen atom, possibly abstracted from residual solvent (1,2-dichloroethane). The second most abundant ion in this spectrum (m/z 212) corresponds to an anion with a composition of $C_{15}O_2$. For all three compounds 1, 2, and 3, the relative abundances of the lower mass fragment ions are enhanced when laser desorption is performed using higher laser power. Different stabilities of C_{18} , C_{24} , and C_{30} have previously been advanced to explain the mass spectra of supersonic beams produced by ultraviolet laser vaporization of graphite.¹⁵ In comparison to the monocyclic structures in the range from C_{10} to C_{29} , carbon ions in the range from C_{30} to C_{40} are very reactive.

Positive Ion Spectra. When one examines the source cell positive ion laser desorption spectra, the presence of carbon aggregate ions, in addition to the expected parent ion fragments, is obvious. Hence, at lower laser intensities, the fully decarbonylated C_{18} (m/z 216) and C_{24} (m/z 288) fragment ions are observed, although with low relative abundances, as are dimer ions with m/z 432 (C_{36}), m/z 576 (C_{48}), and m/z 720 (C_{60}), depending upon the precursor (Figures 8 and 9). Most interestingly, the low-power positive ion LD spectra of $C_{24}O_6$ (1) and $C_{32}O_8$ (2) (Figure 8) also contain relatively abundant contributions from carbon ions formed by laser pyrolysis, including C_{50} , C_{60} , and C_{70} , with other even-numbered higher carbon aggregates separated by 24-Da intervals. All mass spectra were produced with only one laser pulse. This presumably indicates that these larger C_n^+ are not a result of "preformed" species produced by a previous laser pulse which are subsequently desorbed/ionized. The results suggest that these ions are generated from the corresponding cyclocarbons by oligomerizations in the gas phase, followed by successive C_2 losses to form the C_{50} , C_{60} , and C_{70} ions, since both dimers of C_{18} (C_{36}) and C_{24} (C_{48}) are observed, and no significant amount of small carbon ions are present below m/z 216 (C_{18}), and m/z 288 (C_{24}), respectively.

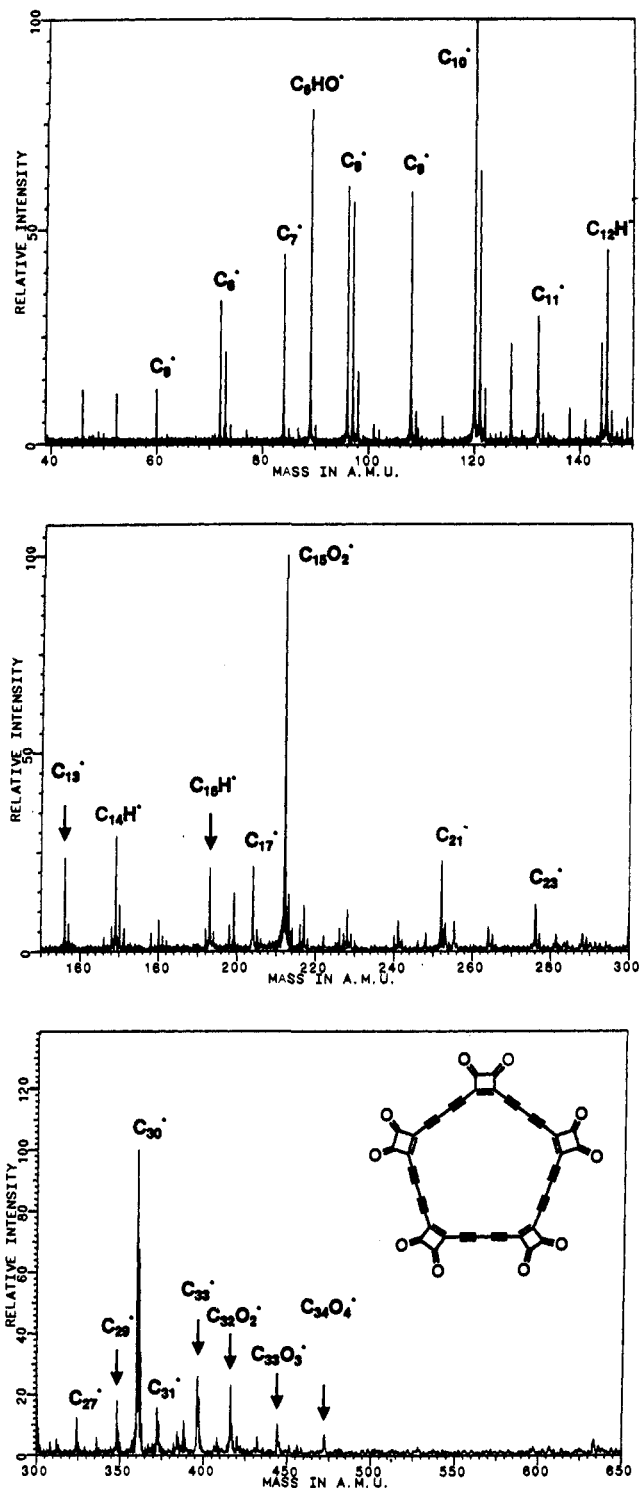


Figure 7. Negative ion laser desorption Fourier transform mass spectrum of carbon oxide 3 at low laser power.

The formation of carbon ions by laser vaporization of graphite has been studied extensively, showing in particular that the C_{60} ion is formed predominantly under certain conditions.¹⁷⁻²⁰

(17) (a) Curl, R. F.; Smalley, R. E. *Science* **1988**, *242*, 1017-1022. (b) Kroto, H. *Science* **1988**, *242*, 1139-1145. (c) Zhang, Q. L.; O'Brien, S. C.; Heath, J. R.; Liu, Y.; Curl, R. F.; Kroto, H.; Smalley, R. E. *J. Phys. Chem.* **1986**, *90*, 525-528.

(18) (a) Röhlfing, E. A.; Cox, D. M.; Kaldor, A. *J. Chem. Phys.* **1984**, *81*, 3322-3330. (b) Cox, D. M.; Reichmann, K. C.; Kaldor, A. *J. Chem. Phys.* **1988**, *88*, 1588-1597.

(19) (a) Kroto, H. W. *Nature* **1987**, *329*, 529-531. (b) Schmalz, T. G.; Seitz, W. A.; Klein, D. J.; Hite, G. E. *J. Am. Chem. Soc.* **1988**, *110*, 1113-1127.

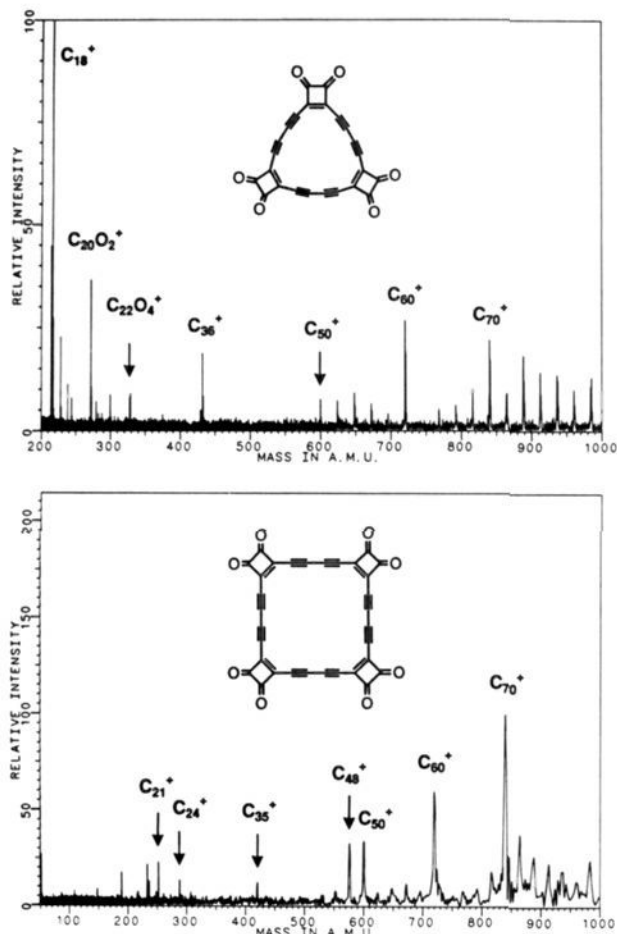


Figure 8. Positive ion laser desorption Fourier transform mass spectra of carbon oxides **1** and **2** at low laser power.

Fragmentation of the higher carbon ions such as C_{60} involves C_2 losses only.^{17c}

In the low-power LD spectrum of $C_{40}O_{10}$ (**3**) (Figure 9, upper spectrum), the abundance of the C_{60} ion (relative to other ions in the spectrum) is significantly greater than in the low-power spectra of the smaller homologues **1** and **2**. We interpret this to reflect both the instability of C_{30} and the dual source of C_{60} ions in this case (i.e., by ion-molecule reaction of C_{30} with the positive ion derived from it and from gas-phase reactions of carbon fragments arising from pyrolysis). When maximum laser power is used, source cell mass spectra of all three parent compounds are essentially the same and simply reflect the pyrolysis and subsequent formation of even-numbered carbon aggregates extending up to at least C_{354} (Figure 9, lower spectrum), as previously observed with carbon-containing precursors as diverse as benzene soot, polymers, and asphaltene.^{21,22}

In conclusion, the novel higher oxides of carbon $C_{24}O_6$ (**1**), $C_{32}O_8$ (**2**), and $C_{40}O_{10}$ (**3**) were isolated and characterized. The X-ray crystal structure of **1** confirms the planarity of this novel system, further supporting conclusions drawn from the electronic absorption spectra of this material. The laser desorption Fourier transform mass spectra of **1** and **2** show a remarkable ease of successive losses of two CO molecules to give C_{18} and C_{24} ions, respectively, in both positive and negative modes. The C_{30} ion is considerably less stable than the smaller homologues, and its formation through fragmentation of **3** is only observed in the negative ion mode. In the positive ion spectra recorded at low

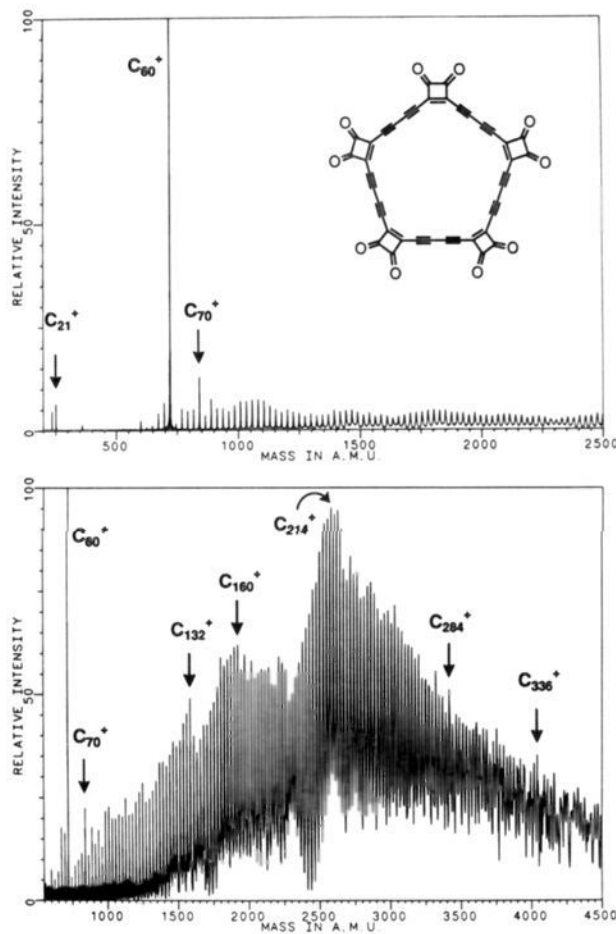


Figure 9. Positive ion laser desorption Fourier transform mass spectrum of carbon oxide **3** at low laser power (above) and at maximum laser power (below). Selected peaks have been labeled as convenient reference points; enhanced stability is not suggested.

desorption laser power, ions corresponding to the dimers of the cyclocarbons are abundant. In addition, higher carbon ions are formed with C_{60}^+ being a prominent ion in the spectra obtained from all three carbon oxides. Although the abundant formation of C_{60}^+ from all three cyclocarbons is remarkable, these results do not tell much about the nature of these ions. The ion distributions at high laser power correlate with previous observations on the laser desorption of graphite and other carbon-rich materials. In addition to C_{60}^+ , carbon ions up to C_{400}^+ are abundant under these conditions in all spectra. The formation of the neutral cyclocarbons by preparative laser desorption of **1-3** in tandem with flash vacuum pyrolysis is currently under investigation. Further studies will be performed to gain more insights into the mechanisms involved in the formation of the higher carbon ions starting from the cyclocarbon ions.

Experimental Section

General. 1H NMR spectra were measured on a Bruker AM360 spectrometer with Me_4Si as internal standard. ^{13}C NMR spectra at 90.6 MHz were taken with the solvent signal as reference unless specified otherwise. All NMR spectra were carried out at 296 K. Melting points were measured on an Electrothermal apparatus and are uncorrected. IR spectra were recorded on a Perkin-Elmer PE 580 apparatus. Electronic absorption spectra were taken on a Varian Cary 2300 spectrometer. Column chromatographies were made on silica gel 230-400 mesh (flash) from E. Merck. Although no exceptional instability was recorded at 25 °C, safety shields were used in all the preparations involving compounds **1-4**. All manipulations with the light-sensitive carbon oxides **1-3** were performed in the dark.

Materials. All reagents and solvents were purchased reagent grade and used without further purification. 1,2-Dichloroethane was dried over molecular sieves 4 Å prior to use.

(20) Ebert, L. B. *Science* **1990**, *247*, 1468-1470.

(21) So, H.; Wilkins, C. L. *J. Phys. Chem.* **1989**, *93*, 1187-1189.

(22) Brown, C. E.; Kovacic, P.; Welch, K. J.; Cody, R. B.; Hein, R. E.; Kinsinger, J. A. *J. Polym. Sci. Part A: Polym. Chem.* **1988**, *26*, 131-148.

Synthesis. Cyclization of 4 to Hexaketel 5, Octaketel 6, and Decaketel 7. A decanted solution of 50 mL (~18 mmol) of Hay catalyst,²³ prepared from 10 g (0.1 mol) of CuCl and 4.18 g (36 mmol) of TMEDA in 100 mL of acetone under argon, was added to a solution of 3.86 g (17.7 mmol) of 4 in 1 L of acetone. The yellow-green solution was stirred vigorously under an atmosphere of dry oxygen (balloon) at 20 °C for 2 h. The solution was filtered through Celite, and the filter cake was washed with 5 × 200 mL of chloroform. The combined filtrates were extracted with 2 × 2 L of water, then dried and evaporated at ≤30 °C in vacuo. The crude solid was purified by flash chromatography with chloroform/acetone (9:1 to 7:3). The first fractions of pure hexaketel 5 were collected and evaporated. The fractions containing mostly octaketel 6, together with some 5 and 7, were combined and evaporated to ~15 mL. The poorly soluble octaketel 6 was filtered off, washed with 3 × 5 mL of dichloromethane, and dried. The filtrates were evaporated and chromatographed again to give additional 5, 6, and 7. The fractions from the first chromatography containing mainly the decaketel 7 were evaporated and chromatographed a second time with the same solvent mixtures to give pure 7 and additional 6. The combined yields were 16.2% for 5, 18.3% for 6, and 6.6% for 7. All three compounds 5, 6, and 7 were identical (¹H and ¹³C NMR, IR) with materials prepared previously in a low total yield (10%).⁴

Deprotection of Ketals 5, 6, and 7 to Carbon Oxides 1, 2, and 3. In a dry 100-mL round-bottomed flask containing a magnetic stirring bar, concentrated (96%) sulfuric acid was dropped onto the ketals 5, 6, or 7 at 25 °C while stirring gently under argon. Approximately 1 mL of H₂SO₄ was used for 50 mg of ketal. After complete dissolution (~5 min), dry 1,2-dichloroethane (~50 mL) was added and the mixture stirred vigorously for 10 min under argon. After allowing the sulfuric acid phase to settle, the upper organic phase was decanted into a second, dry flask under argon, containing dry, powdered CaCO₃ (~2 g) and a stirring bar. Some more dry solvent was added to the first flask to help transfer all material. The clear, colored solutions of the carbon oxides 1 (orange-yellow), 2 (red), or 3 (yellow) were stirred with the calcium carbonate for 10 min and filtered rapidly into a third dry flask. Evaporation under reduced pressure below 30 °C to near dryness, followed by drying at the pump for 15 min in the dark, gave pure materials, too unstable for sending out for element analysis.

Starting from 72.4 mg (0.112 mmol) of 5, 53.7 mg (99%) of red crystals of 1 was obtained, mp >90 °C (*violent explosion*); FT IR (CHCl₃) ν (C≡C) 2129, (C=O) 1791, (C=C) 1539 cm⁻¹; ¹³C NMR, see Table I; UV/vis (1,2-dichloroethane) λ_{max} (nm) 271 sh (ε 19 100), 316 sh (10 100), 339 sh (18 200), 354 (33 200), 359 (33 200), 380 (64 500), 429 (12 700), 437 (13 300), 480 sh (11 70), 511 sh (496), 536 sh (292), 582 sh (170); LD/FTMS, see text. Crystals for X-ray analysis were grown by slow diffusion of *n*-hexane into a solution of 1 in 1,2-dichloroethane over 2 weeks at 25 °C.

Starting from 36.8 mg (0.043 mmol) of 6, 17.3 mg (79%) of 2 was obtained as a red powder, mp >85 °C (*explosion*); IR (CHCl₃) ν (C≡C) 2125, (C=O) 1787, (C=C) 1560 cm⁻¹; ¹³C NMR, see Table I; UV/vis (1,2-dichloroethane) λ_{max} (nm) 264 sh (ε 42 400), 294 (31 900), 355 sh (51 200), 365 (55 300), 399 (66 000), 484 sh (3770), 530 sh (2500), absorption tailing to 770 nm; LD/FTMS, see text.

Starting from 45.0 mg (0.042 mmol) of 7, 24.0 mg (90%) of 3 was obtained as orange yellow needles, mp >85 °C (*explosion*); IR (CHCl₃) ν (C≡C) 2125, (C=O) 1787 cm⁻¹; ¹³C NMR, see Table I; UV/vis (1,2-dichloroethane) λ_{max} (nm) 263 sh (ε 36 700), 331 (36 000), 361 sh

(35 600), 370 (35 700), 415 sh (23 800), 482 sh (9630), absorption tailing to 750 nm; LD/FTMS, see text.

Laser Desorption Fourier Transform Mass Spectrometry. Mass spectra were recorded using a Nicolet FTMS 2000 Fourier transform mass spectrometer interfaced with a Tachisto 215 pulsed TEA CO₂ laser. The spectrometer is equipped with a 7-T superconducting magnet and solids autoprobes and contains differentially pumped source and analyzer cells separated by a 2-mm conductance limit. The CO₂ laser is directed into the mass spectrometer through a zinc selenide window in the source flange and is focused onto the tip of the solids probe to ~1-mm² spot size by an off-axis paraboloid mirror mounted on the source cell assembly. The laser delivers approximately 10⁶ to 10⁸ W/cm² per 80 ± 40 ns pulse.

Spectra were obtained in the direct mode under broad-band excitation and observation conditions. Initially, source cell detection was employed for each of the carbon oxides to obtain negative ion survey spectra. Under these conditions, mass resolution of 1000 to 2000 was routinely obtained. If desired, higher resolution spectra (e.g., 31 000 for *m/z* 512) could also be obtained by transferring trapped ions through the conductance limit for analyzer cell detection, using a 416-μs or longer transfer time (for ions with masses greater than 500 Da). Transfer time corresponds to the length of time the conductance limit is grounded to allow passage of laser-desorbed ions from the source cell into the analyzer cell. No positive ion spectra could be obtained using analyzer cell detection. In an attempt to observe positive ion spectra, source cell detection was investigated. Under a variety of conditions, the positive ion spectra obtained included both contributions from the parent compound and from carbon aggregates formed during the laser desorption process. Absolute trapping voltages of 1.6 V were used for both source cell and analyzer cell in the negative and positive ion experiments. For source cell negative ion survey spectra, following a delay of 8 s after the desorption event to allow desorbed neutrals to be pumped away, ions were excited via a 200-V_{pp} chirp excitation from 0 to 2.66 MHz at 1.33 kHz/μs. Survey spectra of carbon oxides were obtained for each sample following a single laser shot and collecting 128K data points. For higher resolution negative ion analyzer cell spectra, excitation was applied from 0 to 500 kHz at 240 Hz/μs. In each of the high-resolution measurements, four 128K data transients were collected and coadded. For source cell positive ion spectra of carbon oxides, their fragments, and carbon aggregates, 200-V_{pp} chirp excitation from 0 to 500 KHz at 240 Hz/μs was employed. In all cases, the time domain data were augmented by one level of zero filling and fast Fourier transformed to obtain magnitude mode spectra. No apodization was employed.

Sample vials were opened under a nitrogen atmosphere and, for each sample, a 20-μL aliquot of the solution of 1, 2, and 3 in 1,2-dichloroethane was deposited onto a stainless steel probe tip. The solvent was allowed to evaporate under nitrogen in the dark. The coated probe tip was then transferred to the mass spectrometer probe, which was immediately inserted into the vacuum chamber. After insertion of the sample probe into the mass spectrometer source, the background pressure was allowed to drop to about 2–3 × 10⁻⁸ Torr before analysis.

Acknowledgment. We thank the National Science Foundation for support of this work through Grants CHE-89-11685 (CLW) and CHE-89-21133 (FD).

Supplementary Material Available: Experimental details of the crystal structure determinations for 1 and 8 and tables of atomic coordinates, equivalent isotropic thermal parameters, bond angles, and bond lengths (11 pages); listing of structure factors (9 pages). Ordering information is given on any current masthead page.

(23) Jones, G. E.; Kendrick, D. A.; Holmes, A. B. *Org. Synth.* 1987, 65, 52–59.